ELSEVIER

Ceramics International 28 (2002) 741–745

CERAMICS INTERNATIONAL

www.elsevier.com/locate/ceramint

Dielectric and infrared properties of silicon carbide nanopowders

Jingjing Sun*, Jianbao Li, Geliang Sun, Bo Zhang, Shuxia Zhang, Huazhang Zhai

State Key Laboratory of New Ceramics and Fine Processing, Department of Materials Science and Engineering, Tsinghua University, Beijing 100084, PR China

Received 3 August 2001; received in revised form 24 October 2001; accepted 18 February 2002

Abstract

The dielectric properties at high frequencies and infrared spectra of pure, aluminum, and nitrogen-doped SiC nanopowders have been investigated. The powders were prepared by a sol-gel process. Dielectric constants (ϵ') and dielectric loss tangents (tanδ) were measured within the microwave frequency range from 4 to18 GHz. Both ϵ' and tanδ of pure SiC nanopowder are much higher ($\epsilon' = 40$–50, tan$\delta = 0.6$–0.7) than for the doped ones over the frequency range. The dielectric parameters decreased with increasing aluminum and nitrogen contents. Infrared (IR) spectra were measured in the range from 500 to 4000 cm^{-1}, showing that the background of pure SiC nanopowder is also much higher than for the doped ones. The possible mechanisms of these promising features of undoped SiC nanopowder are discussed. © 2002 Elsevier Science Ltd and Techna S.r.l. All rights reserved.

Keywords: A. Sol–gel process; C. Dielectric properties; D. SiC

1. Introduction

Nano materials are drawing increased attention and have been developed extensively in recent years. Nano silicon carbon is well known as a good structural ceramic. Much work has been reported on its synthesis, mechanical properties, heat treatment, and dopant analysis [1–4]. However, little information is available on its dielectric properties, especially at high frequencies for applications in microwave components such as isolators and electromagnetic wave absorbing materials.

Recently, A. Kassiba et al. analyzed the relationship between dielectric behavior and the interfacial polarization of SiC nano-sized materials [5]. Donglin Zhao et al. compared the dielectric properties of nano Si/C/N composite powder with nano SiC powder [6]. But till now, to our knowledge, no work has been reported on the comparison between undoped and doped SiC nanopowders at the microwave frequency range, and the cause of above properties has not been quite clear. So, the purpose of this paper is to study the dielectric as well as infrared spectral properties of pure and doped SiC nanopowders. Possible mechanisms are also discussed.

2. Experimental procedure

SiC nanopowders were synthesized by the carbothermal reduction of SiO_2 and SiO_2–Al_2O_3 xerogels. For the SiO_2–Al_2O_3 xerogels, the initial mixture sol was prepared by mixing tetraethylorthosilicate (TEOS), ethanol, water, saccharose ($C_{12}H_{22}O_{11}$) and some Al_2O_3 powders (with 0.2 μm average particle size). The Al_2O_3 content was varied to study its effect on solid solution formation and properties. Samples composition is listed in Table 1. After stirred for 4 h, the mixture sol was allowed to gel, age and dry at 40 °C for 48 h.

The SiO_2 and SiO_2–Al_2O_3 xerogels were heated at 600 °C for 2 h to carbonize the saccharose, at 1550 °C for 1 h in argon or nitrogen to synthesize SiC (Table 1), at 650 °C in air to remove excess carbon, and finally treated with dilute hydrofluoric acid to remove residual silica.

XRD (D/MAX IIIB, Cu-K_α) was used to analyze the crystalline phases and polytypes of carbothermal reduction products. Lattice definition was carried out with the use of inner 99.99% Si standard (particles size ≈10 μm, $a = 5.43088$ Å). Powders composition was investigated by SEM (JSM-6301F) coupled with EDS, and their morphology and grain sizes were observed by TEM.

The samples for dielectric parameter measurements were prepared by blending the SiC powders with paraffin

* Corresponding author. Tel.: +86-10-6277-3349; fax: +86-10-6278-6911.

E-mail address: sunjingjing00@mails.tsinghua.edu.cn (J. Sun).

0272-8842/02/$22.00 © 2002 Elsevier Science Ltd and Techna S.r.l. All rights reserved.
PII: S0272-8842(02)00037-8

wax in a volume ratio of 1:1.5, and then pressed into $7.00\times3.04\times3$ mm^3 (outer diameter×inner diameter× thickness) rings. Commercially available paraffin wax was used. The dielectric parameters were measured by a network analyzer (HP 8510B) in the frequency range 4–18 GHz. The infrared spectra were recorded at room temperature in the range 500–4000 cm^{-1} by using an infrared spectrometer (model SPECTRUM-GX).

3. Results and discussion

3.1. Synthesis of nanopowders

The XRD patterns of the samples obtained by carbothermal reduction are given in Fig. 1. It is seen from the diffractograms that the products obtained are SiC, whose polytypes are 3C, 12H and 21R. Sample 1 synthesized without Al, contains the 3C (β-SiC) phase. But in the samples doped with Al, the polytypes change to α-type. In detail, samples 2 and 3, reacted in argon, possess the 12H structure; samples 4 and 5, reacted in nitrogen, possess a little more complex structure 21R.

Similar change in SiC polytypes was also observed previously [7,8]. During our synthesis, aluminum atoms enter SiC lattice, replace some silicon atoms and induce carbon vacancies. As a result of this substitution, the (103) reflection emerges as well as (101). Although aluminum has a larger atom radius than silicon, thus making the lattice expand, carbon vacancies lead the lattice to shrink more. These two effects counteract and reduce the lattice parameters as a whole. The lattice parameters calculated from XRD are listed in Table 2, in which a and c decrease with increasing aluminum content. Samples 4 and 5 show larger lattice shrinkage than those synthesized in argon, due to the formation of silicon vacancies in the lattice when nitrogen atoms replace some carbon during reactions in nitrogen.

Table 1
Aluminum content in xerogels in different reaction atmosphere

Sample	Atom ratio of Al to Si	Reaction atmosphere
1	0	Argon
2	2.63:100	Argon
3	5.26:100	Argon
4	2.63:100	Nitrogen
5	5.26:100	Nitrogen

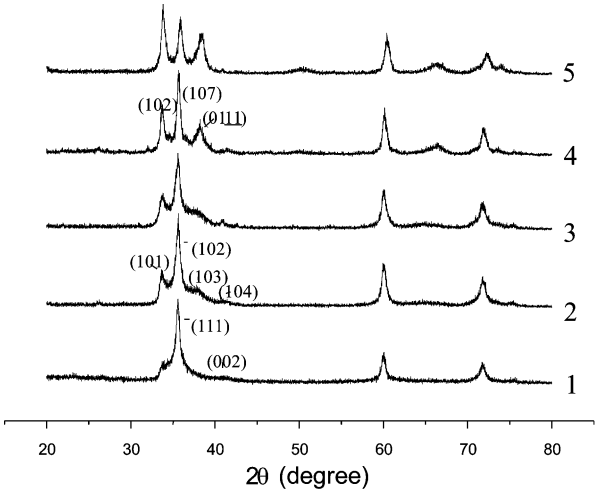

Fig. 1. X-ray diffraction patterns of SiC samples.

The crystallite sizes of the samples were calculated using the Scherrer equation:

$$D_{hkl} = k\lambda/(B_{1/2}\cos\theta) \quad (1)$$

where D_{hkl} is the grain size in the direction perpendicular to the crystal face $\{hkl\}$, k is the Scherrer constant, λ is the X-ray wavelength, $B_{1/2}$ is the half width of the line, and θ is the Bragg's angle of the crystal face $\{hkl\}$. Deducted the possible errors due to the apparatus, the values are listed in Table 2. For all the samples, the grain sizes are in the range of 13–20 nm. The morphology and grain size of all the samples were observed by TEM, which confirmed the value of grain size calculated by XRD. The details have been described in our previous paper [9].

3.2. Dielectric properties

Fig. 2 shows the dielectric constant (ϵ') and dielectric loss tangent (tanδ) of all the samples at the microwave frequency range from 4 to 18 GHz at room temperature. Sample 1 (β-SiC) has the highest dielectric constant as well as dielectric loss tangent. For the other samples, the dielectric constants and dielectric loss tangents are inversely proportional to aluminum content. For the powders with the same aluminum content, the one synthesized in nitrogen has lower values for ϵ' and tanδ than the one synthesized in argon. All the curves show minor changes over the whole frequency range from 4 to 18 GHz.

Table 2
Lattice constants of SiC nanopowders

Sample	Crystalline structure	Grain size (nm)	Standard lattice (Å)	Tested lattice (Å)
1	β(3C)	18.3	$a=4.3589$	$a=4.341$
2	12H	15.2	$a=3.073$	$a=3.070$
			$c=15.080$	$c=15.036$
3	12H	12.9	$a=3.073$	$a=3.062$
			$c=15.080$	$c=14.999$
4	21R	19.4	$a=3.073$	$a=3.049$
			$c=52.78$	$c=52.336$
5	21R	15.2	$a=3.073$	$a=3.026$
			$c=52.78$	$c=51.921$

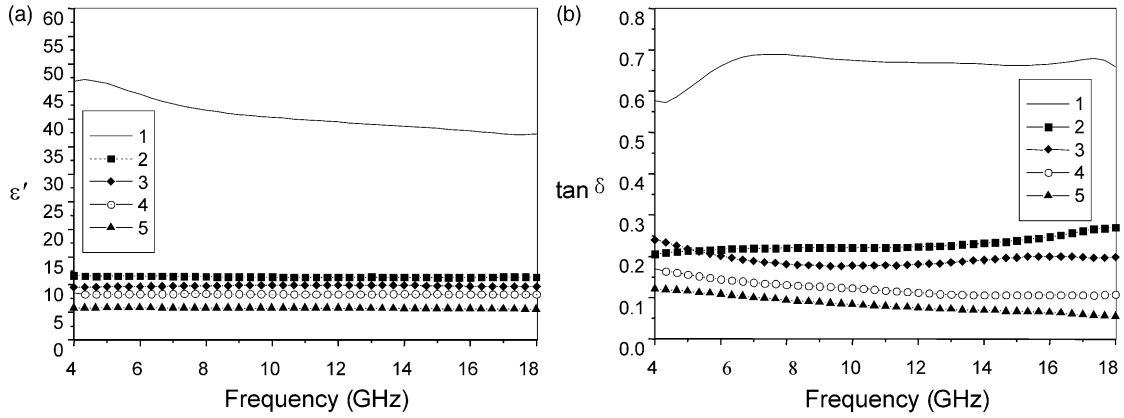

Fig. 2. Dielectric constant ε' (a) and dielectric loss tangent tanδ (b) of studied samples.

Because SiC is a non-magnetic material ($\mu'_r = 1$, $\mu''_r = 0$), its power dissipation is only determined by dielectric losses. Dielectric losses usually result from three primary processes: ion migration losses [including (a) dc conductivity losses and (b) ion jump and dipole relaxation losses], ion vibration and deformation losses, and electron polarization losses [10]. Dc conductivity losses are usually important for many dielectric materials, so this is discussed first. In the doped samples, aluminum and nitrogen atoms will substitute Si and C atoms respectively. Except native ones, possible defect reactions are:

$$\mathrm{Al} \xrightarrow{\mathrm{SiC}} \mathrm{Al}'_{\mathrm{Si}} + h^{\cdot} \tag{2}$$

$$\mathrm{Al_4C_3} \xrightarrow{\mathrm{SiC}} 4\mathrm{Al}'_{\mathrm{Si}} + 3\mathrm{C_C} + V_{\mathrm{C}}^{\cdot\cdot\cdot} \tag{3}$$

$$\mathrm{N} \xrightarrow{\mathrm{SiC}} \mathrm{N}_{\mathrm{C}}^{\cdot} + e' \tag{4}$$

$$\mathrm{AlN} \xrightarrow{\mathrm{SiC}} \mathrm{Al}'_{\mathrm{Si}} + \mathrm{N}_{\mathrm{C}}^{\cdot} \tag{5}$$

$$\mathrm{Al_2O_3} \xrightarrow{\mathrm{SiC}} 2\mathrm{Al}'_{\mathrm{Si}} + 3\mathrm{O}_{\mathrm{C}}^{\cdot\cdot} + V_{\mathrm{Si}}'''' \tag{6}$$

In detail, reactions (2), (3) and (6) may exist in the SiC synthesis in argon, and reactions (2), (4), (5) and (6) may exist in the synthesis in nitrogen. The substitution of silicon atoms by aluminum leads to an acceptor level within the band gap and the conductivity is due to holes. Therefore, the conductivities of SiC powders in argon simply increase with increasing aluminum content. Similarly, the substitution of silicon atoms by nitrogen leads to an electron donor level and the conductivity is due to electrons. When Al and N both exist, although the concentration of carriers will decrease because of the two kinds of carriers with contrary charges, the drift mobility of carriers is the sum of these two kinds of carriers. As a result of the higher carrier mobility, the SiC conductivities in nitrogen should be much higher than those of SiC in argon. Table 3 lists the dc conductivities of the SiC samples, showing that the conductivity changes are in agreement with the above analysis, namely the conductivities of samples 4 and 5 are respectively larger than those of samples 2 and 3.

If the dielectric loss tangent only results from electrical conductivity, it should obey the following formula [10]:

$$tg\delta_{\mathrm{C}} = \frac{\sigma}{2\pi f \varepsilon'_{\mathrm{r}} \varepsilon_0} = \frac{\sigma}{(8.85 \times 10^{-14}) 2\pi f \varepsilon'_{\mathrm{r}}} \tag{7}$$

here the conductivity is given in ohm-cm^{-1}. The loss tangent for the SiC samples at 10 GHz is also calculated in Table 3. The ϵ'_r values for samples containing 40 vol.% SiC powder are simply adopted in this equation. It should be noted that the true value of ϵ'_{r} is much higher than the measured one and can be inferred according to the mixture rules. So the practical tanδ_{c} should be less than the calculated one. In contrast, the loss tangent of samples 2–5 decreases with increasing conductivity. In particular, the loss tangent of sample 1 is much higher than that for other samples though samples 4 and 5 have higher conductivities. All these phenomena contradict with the results calculated from the Eq. (7), indicating that conductivity losses are not the main cause of the dielectric losses in our study.

Table 3
dc Conductivity and calculated loss tangent[a] of SiC samples

Sample	dc Conductivity (S cm^{-1})	Calculated loss tangent for 10 GHz
1	1.79×10^{-3}	8.00×10^{-2}
2	5.54×10^{-4}	8.78×10^{-2}
3	1.96×10^{-3}	3.57×10^{-1}
4	8.46×10^{-4}	1.84×10^{-1}
5	1.30×10^{-2}	4.06×10^{-1}

[a] The values are calculated for pure SiC samples.

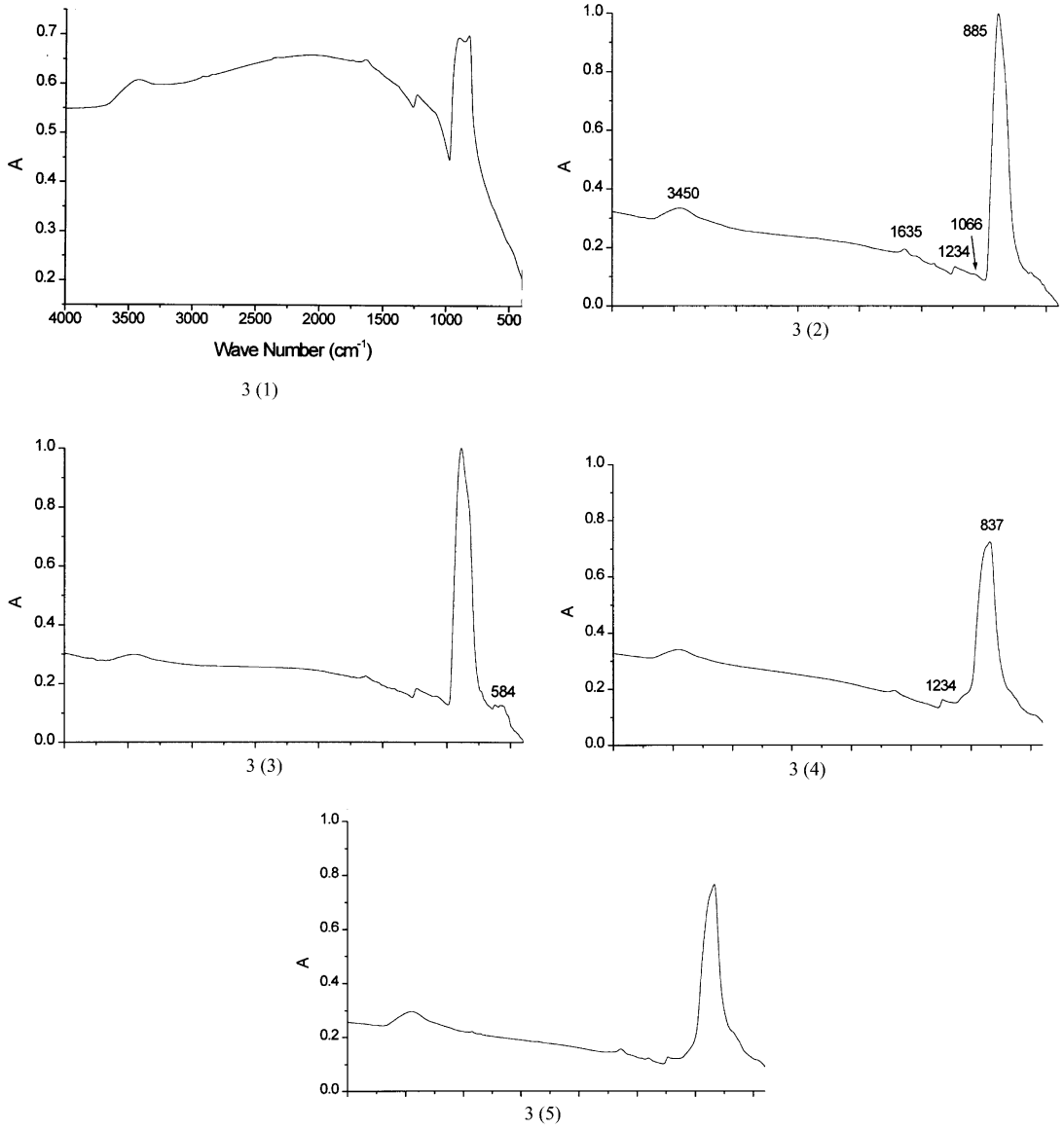

Fig. 3. (1)–(5) IR spectra of SiC samples 1–5.

Ion jump and dipole relaxation may have a crucial effect on the samples' dielectric behavior. In 3C-SiC, the silicon and carbon vacancies (V_{Si}, V_C) as well as silicon and carbon antisites (Si_C, C_{Si}) are the most energetically preferred among native SiC defects preserving a tetrahedral symmetry [11,12]. The defects with opposite charges have a strong trend to form pairs because of static attraction. These defect pairs can be treated as dipoles. The more the dipoles, the higher the dielectric constant is. Under the external alternating electric field, the reorientation of lattice defect pairs results in polarization and energy dissipation. In this case, high relative dielectric constant means high dielectric loss because the reorientation must be completed by the migration of ions, which dissipates energy. This should be the reason why sample 1 possesses highest ϵ' and tanδ. When doped into SiC, aluminum atoms occupy the sites of silicon atoms and reduce the number of those defect pairs. Although aluminum atoms may also partner with the defects with opposite charge, it is more difficult for such defect pairs to reorient because aluminum has a larger covalent atom radius than silicon. The number of defect pairs taking part in polarization decreases with increasing aluminum content, so the conductivity of SiC nanopowders increases, but ϵ' and tanδ decrease. Nitrogen atoms play a similar role and lead to a larger reduction in ϵ' and tanδ.

3.3. Infrared spectra

The IR spectra are given in Fig. 3 (1)–(5). The bands around 800–900 cm^{-1} are attributed to the vibration of the Si–C bond. The value of Si–C absorption bond is higher than that around 700–800 cm^{-1} [13,14]. The dif-

ference should be due to solid solution of aluminum and nitrogen in the SiC powders. The figures also show that the band in samples 2 and 3 (885 cm^{-1}) are slightly higher than for samples 4 and 5 (837 cm^{-1}), which indicates a difference in the crystal conditions around the Si–C bond. The results can be explained by the partial substitution of carbon atoms by nitrogen, thus disturbing the previous lattice order. Compared with the pure SiC powder, aluminum plays a similar role of disturbing the Si–C bond.

The weak bands around 1234 and 1066 cm^{-1} are attributed to the Si–O bond, indicating the existence of a SiO_2 surface on all the samples. The weak bands around 3450 and 1635 cm^{-1} are attributed to H_2O band, caused by water absorption of samples.

A comparison of Fig. 3 (1) with 3 (2)–(5) shows that the absorption background of pure SiC nanopowder is much higher than for the other four spectra. The absorption degree of the background from 1000 to 4000 cm^{-1} in pure SiC powder is comparable with that of the Si–C bond, Whereas in most cases (such as in the other four samples), the degree of background is much weaker than those of main peaks. This interesting result is probably due to the ion vibration and deformation of the pure SiC nanopowder in the infrared range. Furthermore, close examination of IR absorption values reveals that the Si–C band in Fig. 3(1) is slightly split which may relate to the crystallinity rate of the samples [8]. This indicates that the pure SiC powder has a better crystallinity than the other samples doped with aluminum and nitrogen, which is in agreement with the result in XRD that the main peak intensity of sample 1 is the highest.

4. Conclusions

(1) The dielectric properties of pure and doped SiC nanopowders synthesized by the carbothermal reduction of SiO_2 and SiO_2–Al_2O_3 xerogels were measured at the microwave frequency range of 4–18 GHz. The dielectric constant ($\epsilon' = 40$–50) and loss tangent ($\tan\delta = 0.6$–0.7) of pure powder are much higher than for powders doped with aluminum and nitrogen. The promising features of pure SiC nanopowder may be due to ion jump and dipole relaxation in the GHz frequency range, namely the reorientation of lattice defect pairs (V_{Si}–V_C, Si_C–C_{Si}).

(2) Infrared spectra of all the samples were also measured in the range of 500–4000 cm^{-1}. The pure SiC nanopowder has much higher background due to ion vibration and deformation as well as a better crystallinity than powders doped with aluminum and nitrogen.

Acknowledgements

This research was supported by The Open Project Foundation of the State Key Laboratory of New Ceramics and Fine Processing in Tsinghua University (Project No. KF0003).

References

[1] Y. Inomata, H. Tanaka, Y. Inoue, K. Kawabata, Phase relation in SiC–Al_4C_3–B_4C system at 1800 °C, J. Ceram. Soc. Jpn. 88 (1980) 353–355.
[2] V.D. Krstic, Production of fine, high-purity beta-silicon carbide powders, J. Am. Ceram. Soc. 75 (1992) 170–174.
[3] V. Rama, O.P. Bahl, U. Dhawan, Synthesis of silicon carbide through the sol–gel process from different precursors, J. Mater. Sci. 30 (1995) 2686–2693.
[4] R. Zhou, Zh. Feng, Y. Liang, et al., Reactions between SiC and sintering aids in Si_3N_4/SiC nanocomposites and their consequences, Ceramics International 27 (2001) 571–576.
[5] A. Kassiba, M. Tabellout, Conduction and dielectric behaviour of SiC nano-sized materials, Solid State Commun. 115 (2000) 389–393.
[6] A. Kassiba, M. Tabellout, Conduction and dielectric behaviour of SiC nano-sized materials, Solid State Commun. 115 (2000) 389–393.
[7] Y. Sugahara, K.I. Sugimoto, H. Takagi, The formation of SiC–AlN solid solution by the carbothermal reduction process of montmorillonite, J. Mater. Sci. Lett. 7 (7) (1988) 795–797.
[8] A. Julbe, A. Larbot, Ch. Guizard, L. Cot, Effect of boric acid addition in colloidal sol–gel derived SiC precursors, Mater. Res. Bull. 25 (1990) 601–609.
[9] B. Zhang, J.B. Li, J.J. Sun, Solid solution of Al and N in nano-sized α-SiC powders by carbothermal reduction of the xerogels of SiO_2–Al_2O_3, Mater. Lett., in press. Reference No. MLBLUE 3130.
[10] W.D. Kingery, H.K. Bowen, D.R. Uhlmann, Introduction to Ceramics, John Wiley & Sons, New York, 1976, p. 937.
[11] C. Wang, J. Bernholc, R.F. Davis, Formation energies, abundances, and the electronic structure of native defects in cubic SiC, Phys. Rev. B 38 (1988) 12752–12755.
[12] J. Bernholc, S.A. Kajihara, C. Wang, Theory of native defects, doping and diffusion in diamond and silicon carbide, Mater. Sci. Eng. B B11 (1992) 265–272.
[13] X.C. Xiao, Y.W. Li, Structural analysis and microstructural observation of SiC_xN_y films prepared by reactive sputtering of SiC in N_2 and Ar, Appl. Surface Sci. 156 (1–4) (2000) 155–160.
[14] H. Hobert, J.H. Dunken, Infrared and Raman spectroscopic investigation of thin films of AlN and SiC on Si substrates, Vibrational Spectroscopy 19 (2) (1999) 205–211.